JOURNAL OF MATERIALS SCIENCE 15 (1980) 309–326

Surface dislocation model of a dislocation in a two-phase medium

K. JAGANNADHAM, M. J. MARCINKOWSKI
Engineering Materials Group, and Department of Mechanical Engineering, University of Maryland, College Park, Maryland 20742, USA

The surface dislocation method developed earlier for solving the free surface boundary problem is now extended to the two-phase interface boundary problem wherein a lattice dislocation is situated in one of the phases. The interface is planar where two semi-infinite half spaces of different elastic properties are joined. The interface consists of four surface arrays of dislocations, two in each phase, so that the continuity of two stress components and two displacement components is maintained. The continuous distribution of dislocations is employed to arrive at the distribution function representing the surface arrays. The Airy stress functions for the two phases are derived and shown to give the same result as that obtained earlier by other methods. The distortions involved across the interface are represented in terms of simple surface arrays to show the advantage of the surface dislocation model. The stress field around the dislocation in the two-phase medium is plotted and the effect of the shear modulus of the second phase and of Poisson's ratio discussed. The advantages of applying the surface dislocation model either by the continuous distribution method or the discrete dislocation method are indicated.

1. Introduction

The elastic properties of a dislocation in an infinite homogeneous medium can be obtained by solving the elasticity equations with suitable boundary conditions placed on the stresses and displacement [1]. While this method is easily applicable for simple straight configurations of dislocations, the analysis becomes tedious for most complex configurations of dislocations. The Green's function method has been used to solve the problem of curved dislocations [2]. The Green's functions of elasticity are the tensor quantities for the elastic displacements produced due to a point force. These satisfy the elasticity equations for the point force applied on the body. When a dislocation is created in the presence of a point force, there is no cross term in the elastic energy between the stress field of the dislocation and the stress field due to the point force, and since the dislocation is not a sink of energy, the entire energy expended in creating the dislocation configuration is equated to the work done by the point forces. This equality leads to the familiar displacement equations of Burgers [3]. It is therefore imperative that the Green's functions of the displacements are available and therefore the elasticity equations are already solved in a form suitable for further use in summing over the cut surfaces required to produce the dislocation. When the dislocation is situated in a finite medium or a two-phase medium, additional boundary conditions appear. There are various methods used for deriving the elasticity properties of dislocations in these particular cases required to satisfy the boundary conditions.

In the Green's function method extended to two-phase geometry, the elasticity equations are solved for the two-phase medium to obtain the Green's function satisfying the boundary condition [4, 5]. These Green's functions are then used to arrive at the stresses and displacements due to a dislocation in a two-phase medium. In order to satisfy the boundary conditions across the interface, namely the continuity of stresses and displacements, a suitable combination of point forces is chosen and the stresses and displacements are obtained by integration over the cut surfaces

0022–2461/80/020309–18$03.80/0

[6]. In the image dislocation model [7–9], suitable image dislocations are chosen in the two phases in order to satisfy the continuity of stresses and displacements. However, in this case, there are no general rules which specify the choice of the Burgers vectors of the image dislocations required to satisfy the boundary conditions. Thus, the Green's function method is more general and applicable to various geometries, although the mathematics involved may become tedious. A more powerful and straightforward technique which has hitherto been applied to a limited extent is the surface dislocation model used to satisfy the boundary conditions [10]. In this method dislocation arrays with suitable orientations of Burgers vectors are chosen across the interface in the two media to satisfy the boundary conditions. The simplicity of this method enables it to be applied to complex geometries, though not in an analytical form, but replaced by numerical and computational methods. Since the surface dislocation array chosen is real, it explains the geometrical connection between the two phases that constitute the system. This method can be applied not only to internal stresses inside the medium but also to externally applied stresses. Since, a dislocation is an elastic entity whose elastic properties are derived in a homogeneous medium by solving the elasticity equations, the surface dislocation model in effect superimposes the dislocation arrays so as to satisfy the boundary conditions, and thus it is based on the same principle as the Green's function method, although the latter involves, as a first step, solving the elasticity equations for the two-phase medium. The surface dislocation model avoids the tedious mathematics involved in solving elasticity equations for the two-phase medium.

It should also be pointed out that, hitherto, dislocations in two-phase media are treated assuming that the two phases are made of continua. Thus, the structure of the interface is not clearly specified. However, when the two phases with different lattice parameters are joined together, the structure of the interface consists of interface dislocations and misfit dislocations. The interface dislocations have a Burgers vector which is equal to the lattice parameter difference of the two phases. The misfit dislocations are situated periodically within the phase with smaller lattice parameter and their presence decreases the stress field around the interface array and thus makes it short range.

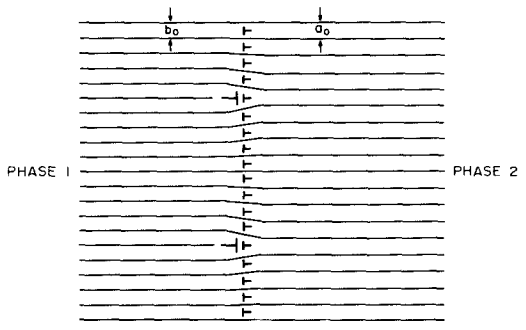

Figure 1 Interface dislocation array and misfit dislocation array shown at the interface of a two-phase system. The extra half plane of the dislocations in the misfit array is situated in phase 1 with smaller lattice parameter. The extra half plane of the interface array is situated in phase 2 with larger lattice parameter. These two arrays are opposite in sign.

Fig. 1 shows the arrangement of the interface dislocations and misfit dislocations before rearrangement of the interface array under the attractive force of the misfit array, the mutual repulsive force of the interface dislocations and the frictional stress acting along the interface. The resulting arrangement leads to a partially coherent interface [11]. When an extraneous dislocation is now introduced into any one of the two phases, the surface dislocation model can be used to satisfy the internal surface boundary conditions. These surface dislocations, which will be introduced shortly to satisfy the continuity of stresses and displacements, are in addition to the already existing interface and misfit dislocation arrays. The interface dislocation arrays are defined so as to accommodate the lattice difference between the two phases, while the surface dislocation arrays are used to maintain the continuity conditions across the interface. In further analysis below, the interface dislocations and misfit dislocations are not considered, but the surface dislocation distributions required to satisfy the continuity conditions across the interface are determined.

2. Surface dislocation models

The surface dislocation model has a wide range of applications and it is one of the methods that can be used to satisfy the boundary conditions in problems of elasticity. This method can be used when both external and internal stresses are present [10, 12]. In the following, a two-phase medium with phases possessing different elastic properties will be considered to be joined across a

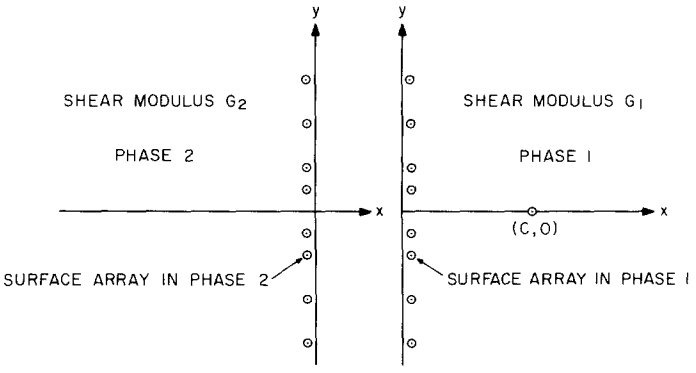

Figure 2 The two elastic half spaces with different elastic properties shown before joining together to form the two-phase system. The right-hand half space contains a dislocation with the surface array. The left-hand half space contains a surface array which brings the stress and displacement field to a level equal to that on the surface of the right-hand side.

planar interface. One of the two phases will contain a dislocation. The surface arrays in the two phases required to satisfy the continuity of stresses and displacements across the interface will be obtained and the stresses and displacements due to the arrays evaluated.

Consider, as shown in Fig. 2, two elastic half spaces with different elastic properties, which are separated from each other. The right-hand side consists of phase 1 with a screw dislocation of Burgers vector b_s along the z direction situated at $(c, 0)$ from the surface. The surface array of screw dislocations placed on the surface brings the stresses on the surface to a value which depends on the y coordinate. The left-hand side consists of phase 2 with a surface array of screw dislocations which brings the stresses and displacements or displacement gradient in the y direction to the same value as that on the surface of the right-hand side half space. Therefore the two half spaces are separate although the stresses and displacements are made to coincide on the surface. When the two half spaces are now joined, the two-phase medium containing the dislocation in phase 1 forms the surface dislocation model, as shown in Fig. 3. In Fig. 3, the array to the right of the interface belongs to phase 1 completely, and that to the left to phase 2 completely. The elastic properties of each of these surface arrays are obtained by considering them to be situated in an infinite medium of the phase in which they are present. The interface arrays discussed earlier are different from the surface array in the sense that the interface array introduced distortion in both the phases, but the surface array in each phase has a distortion only in that phase. The continuous distribution of these two surface arrays is determined by using the continuity of the σ_{xz} component of stress and the U_z component of displacement.

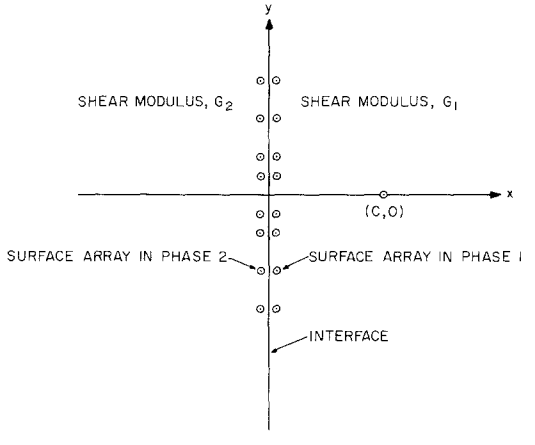

Figure 3 Surface dislocation model required to satisfy the continuity of the σ_{xz} component of stress and the U_z component of displacement across the interface. The lattice dislocation is situated in phase 1 at $(c, 0)$. Each surface array belongs to the phase in which it is present.

Fig. 4 shows an edge dislocation of Burgers vector b_s perpendicular to the interface and situated at $(c, 0)$ in phase 1. The formation of the two-phase system containing an edge dislocation can be visualized in the same way as that of a screw dislocation. In order to satisfy the continuity of two stress components σ_{xx} and σ_{xy} and the two displacement components U_x and U_y, two dislocation arrays of the same character as the lattice dislocation, but with Burgers vector b_{x_i}, are placed in the two phases and two more with Burgers vector b_{y_i}, parallel to the interface, are placed in the two phases. Thus, there are two arrays in each phase and four arrays in both the phases combined which are needed to satisfy the continuity of stresses and of displacements. It should be noted from Fig. 4 that one of the arrays changes its sign along the y axis while the other has the same sign in the positive and negative y

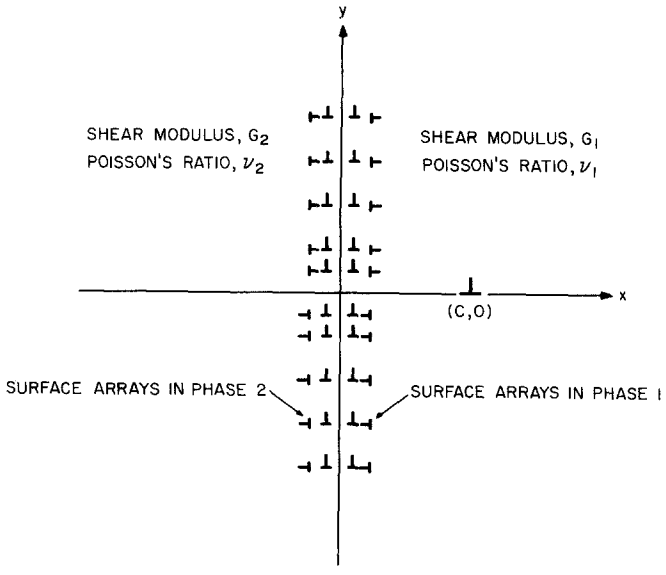

Figure 4 Surface dislocation model required to satisfy the continuity of the σ_{xx} and σ_{xy} components of stress and the U_x and U_y components of displacement. Two arrays are required in each phase, one with Burgers vector parallel to the interface and the other with Burgers vector perpendicular to the interface. The lattice dislocation is situated in phase 1 at $(c, 0)$ with Burgers vector perpendicular to the interface.

axis. The exact nature of these dislocation arrays will become evident from their corresponding distribution functions. Fig. 5 shows an edge dislocation whose Burgers vector b_s is parallel to the interface and situated at $(c, 0)$ in phase 1. The surface arrays required to satisfy the continuity of stresses and displacements are also shown. It is seen that there are two arrays in each phase, with one of the arrays of the same sign along the y axis and the second array which changes it sign along the y axis.

Thus, the elastic field in a body comprising two different isotropic elastic media, meeting at an interface and one of them, namely phase 1, containing a dislocation, is obtained in this paper. The elastic field in phase 1 extending to infinity beyond the interface is the sum of the elastic field of the dislocation and that of the two distributions of virtual infinitesimal dislocations at the interface in phase 1. The elastic field in phase 2 extending to infinity beyond the interface is the elastic field of the two distributions of virtual infinitesimal dislocations at the interface in phase 2. The requirement of equality of displacements and certain stress components at the interfaces, enabling the virtual extensions of the two media to be cut away, and the real parts of the media to be joined at the interface, gives enough equations to determine the dislocation densities in the four virtual arrays. In the case of a planar interface,

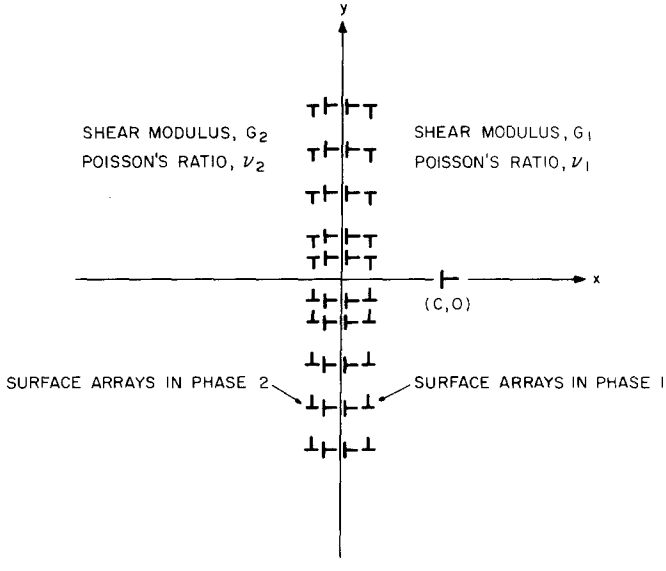

Figure 5 Same as Fig. 4 except that the lattice dislocation has the Burgers vector parallel to the interface.

extending to infinity, these equations are solved. In other cases, where closed form solutions are not obtained, the continuous arrays of infinitesimal virtual dislocations may be replaced by a finite number of discrete virtual dislocations, but no results of this are presented here. In all the figures illustrated in the paper, the discrete dislocations are used to symbolize the continuous arrays of infinitesimal dislocations. In the following, the three orientations of Burgers vector of the dislocation in phase 1 are considered and the elastic fields determined in both phases.

3. A screw dislocation in a two-phase medium

The continuity conditions for a screw dislocation in a two-phase medium, as shown in Fig. 3, can be written in terms of the distribution functions of the two arrays present along the interface. The stress field of the screw dislocation of Burgers vector b_s in an infinite homogeneous medium with shear modulus G_1 can be written as

$$\sigma_{xz} = -\frac{G_1 b_s}{2\pi} \frac{y}{y^2 + (x-c)^2}.$$

$$\sigma_{yz} = \frac{G_1 b_s}{2\pi} \frac{(x-c)}{(x-c)^2 + y^2}.$$

The U_z component of displacement of the dislocation is

$$U_z = \frac{b_s}{2\pi} \tan^{-1}\left(\frac{y}{x-c}\right)$$

These expressions can also be used with suitable modifications for the dislocations in the two surface arrays. Let the distribution function representing the array in phase 1 be $f_1(y_1)$ and that in phase 2 be $f_2(y_1)$. The continuity of σ_{xz} across the interface can be written in the form

$$\frac{G_1 b_i}{2\pi} \int_{-\infty}^{\infty} \frac{f_1(y_1)\,dy_1}{y - y_1} + \frac{G_1 b_s}{2\pi} \frac{y}{y^2 + c^2} =$$

$$\frac{G_2 b_i}{2\pi} \int_{-\infty}^{\infty} \frac{f_2(y_1)\,dy_1}{y - y_1}, \qquad -\infty < y < \infty \tag{1}$$

The continuity of the U_z component of displacement or the gradient of U_z with y across the interface can be written as

$$b_i f_1(y_1) + b_i f_2(y_1) = \frac{b_s}{\pi} \frac{c}{c^2 + y_1^2} \tag{2}$$

Inversion of the integral Equation 1 gives

$$G_1 b_i f_1(y_1) - G_2 b_i f_2(y_1) = -\frac{G_1 b_s}{\pi} \frac{c}{c^2 + y_1^2} \tag{3}$$

Equations 2 and 3 can be solved to obtain

$$f_1(y) = \frac{b_s}{b_i \pi} \left(\frac{G_2 - G_1}{G_2 + G_1}\right) \frac{c}{c^2 + y^2} \tag{4}$$

$$f_2(y) = \frac{2b_s}{b_i \pi} \frac{G_1}{G_2 + G_1} \frac{c}{c^2 + y^2} \tag{5}$$

The stress field due to the array corresponding to the distribution function $f_1(y)$ is given by integrating the stress field of the dislocation in the array over the distribution, which gives,

$$\sigma_{xz_1} =$$

$$-\frac{G_1 b_s}{2\pi} \left(\frac{G_2 - G_1}{G_2 + G_1}\right) \frac{y}{(x+c)^2 + y^2}, \qquad x > 0$$

Similarly, the stress field due to the array corresponding to the distribution function $f_2(y)$ is given by

$$\sigma_{xz_2} =$$

$$-\frac{G_1 b_s}{2\pi} \frac{2G_2}{G_2 + G_1} \frac{y}{(x-c)^2 + y^2}, \qquad x < 0$$

In phase 1, the sum of the stress field of the lattice screw dislocation with Burgers vector b_s and the stress field due to the array, σ_{xz_1} gives

$$\sigma_{xz} =$$

$$-\frac{G_1 b_s}{2\pi} \left[\frac{y}{y^2 + (x-c)^2} + \left(\frac{G_2 - G_1}{G_2 + G_1}\right) \frac{y}{y^2 + (x+c)^2}\right]$$

$$x > 0 \tag{6}$$

The stress field in phase 2 is due to the array given by $f_2(y)$,

$$\sigma_{xz} =$$

$$-\frac{G_1 b_s}{2\pi} \left(\frac{2G_2}{G_2 + G_1}\right) \frac{y}{(x-c)^2 + y^2}, \qquad x < 0 \tag{7}$$

The displacement U_z in both the media are similarly given by

$$U_z = \frac{b_s}{2\pi}\left[\tan^{-1}\left(\frac{y}{x-a}\right)\right.$$

$$\left.+\left(\frac{G_2-G_1}{G_2+G_1}\right)\tan^{-1}\left(\frac{y}{x+a}\right)\right], \quad x>0$$

$$U_z = \frac{b_s}{2\pi}\frac{2G_1}{G_2+G_1}\tan^{-1}\left(\frac{y}{x-a}\right), \quad x<0 \tag{8}$$

It is useful to determine the total Burgers vector of dislocations placed across the interface in both phases. Summing the distribution functions in the y direction gives

$$\int_{-\infty}^{\infty} b_i f_1(y)\,dy = \left(\frac{G_2-G_1}{G_2+G_1}\right)b_s$$

$$\int_{-\infty}^{\infty} b_i f_2(y)\,dy = \left(\frac{2G_1}{G_2+G_1}\right)b_s \tag{9}$$

It is verified from Equations 6, 7 and 8 that the continuity of stresses and displacements is satisfied and these results agree with those obtained from the image dislocation model [9].

4. An edge dislocation in a two-phase medium

4.1. Edge dislocation with Burgers vector perpendicular to the interface

The continuity of stresses and displacements across the interface when the edge dislocation with Burgers vector perpendicular to the interface is considered, as shown in Fig. 4, can be written in terms of the four distribution functions. Let $f_1(y)$ and $f_2(y)$ be the dislocation distribution functions representing the surface arrays whose Burgers vectors, b_{y_i} are parallel to the interface and situated in phase 1 and phase 2 respectively. Similarly, let $f_3(y)$ and $f_4(y)$ be the dislocation distribution functions representing the surface array whose Burgers vector, b_{x_i} are perpendicular to the interface and situated in phase 1 and phase 2 respectively. Across the interface, the σ_{xy} component due to surface arrays given by $f_3(y)$ and $f_4(y)$ is zero. Similarly, the σ_{xx} component due to surface arrays $f_1(y)$ and $f_2(y)$ is zero. Therefore, the continuity of the σ_{xy} component can be written using the stress field expressions in an infinite homogeneous medium [13] and thus takes the form,

$$\frac{G_1 b_{y_i}}{\pi(k_1+1)}\int_{-\infty}^{\infty}\frac{f_1(y_1)\,dy_1}{y-y_1} - \frac{G_2 b_{y_i}}{\pi(k_1+1)}\int_{-\infty}^{\infty}\frac{f_2(y_1)\,dy_1}{y-y_1}$$

$$= \frac{G_1 b_s}{\pi(k_1+1)}\left[\frac{c}{c^2+y^2} - \frac{2c^3}{(c^2+y^2)^2}\right]$$

where $k_1 = 3-4\nu_1$ and $k_2 = 3-4\nu_2$. Inversion of the above equation gives

$$\frac{G_1 f_1(y_1)}{(k_1+1)} - \frac{G_2 f_2(y_1)}{(k_2+1)} = \frac{2G_1 b_s}{\pi(k_1+1)b_{y_i}}\frac{c^2 y}{(c^2+y^2)^2} \tag{10}$$

Similarly, the continuity of the σ_{xx} component can be written in the form,

$$\frac{G_1 b_{x_i}}{\pi(k_1+1)}\int_{-\infty}^{\infty}\frac{f_3(y_1)\,dy_1}{y-y_1} - \frac{G_2 b_{x_i}}{\pi(k_2+1)}\int_{-\infty}^{\infty}\frac{f_4(y_1)\,dy_1}{y-y_1}$$

$$= -\frac{G_1 b_s}{\pi(k_1+1)}\left[\frac{y}{c^2+y^2} + \frac{2c^2 y}{(c^2+y^2)^2}\right]$$

Inverting the above equation,

$$\frac{G_1 f_3(y_1)}{(k_1+1)} - \frac{G_2 f_4(y_1)}{(k_2+1)} = -\frac{2G_1 b_s}{\pi(k_1+1)b_{x_i}}\frac{c^3}{(c^2+y^2)^2} \tag{11}$$

The continuity of the U_y component of displacement or the gradient of U_y in the y direction is written as

$$b_{y_i} f_1(y_1) + b_{y_i} f_2(y_1) - \frac{(k_1-1)b_{x_i}}{\pi(k_1+1)}\int_{-\infty}^{\infty}\frac{f_3(y_1)\,dy_1}{y-y_1}$$

$$+\frac{(k_2-1)b_{x_i}}{\pi(k_2+1)}\int_{-\infty}^{\infty}\frac{f_4(y_1)\,dy_1}{y-y_1}$$

$$= \frac{b_s}{\pi}\left[\left(\frac{k_1-1}{k_1+1}\right)\frac{y}{c_2+y^2} - \frac{4c^2 y}{(k_1+1)(c^2+y^2)^2}\right] \tag{12}$$

Similarly, the continuity of the U_x component of displacement or the gradient of U_x in the y direction is written as

$$b_{x_i} f_3(y_1) + b_{x_i} f_4(y_1) + \frac{(k_1 - 1) b_{y_i}}{\pi(k_1 + 1)} \int_{-\infty}^{\infty} \frac{f_1(y_1)\,dy_1}{y - y_1}$$

$$- \frac{(k_2 - 1) b_{y_i}}{\pi(k_2 + 1)} \int_{-\infty}^{\infty} \frac{f_2(y_1)\,dy_1}{y - y_1}$$

$$= \frac{b_s}{\pi} \left[\left(\frac{k_1 - 1}{k_1 + 1} \right) \frac{c}{c^2 + y^2} + \frac{4c^3}{(k_1 + 1)(c^2 + y^2)^2} \right] \tag{13}$$

Equations 10 to 13 can be solved to arrive at the dislocation distributions. The distribution functions can be assumed to be

$$b_{y_i} f_1(y) = A_1 \frac{y}{c^2 + y^2} + B_1 \frac{c^2 y}{(c^2 + y^2)^2}$$

$$b_{y_i} f_2(y) = A_2 \frac{y}{c_2 + y^2} + B_2 \frac{c^2 y}{(c^2 + y^2)^2}$$

$$b_{x_i} f_3(y) = A_3 \frac{c}{c^2 + y^2} + B_3 \frac{c^3}{(c^2 + y^2)^2}$$

$$b_{x_i} f_4(y) = A_4 \frac{c}{c^2 + y^2} + B_4 \frac{c^3}{(c^2 + y^2)^2} \tag{14}$$

Using Equations 10 to 13 to evaluate the constants provides

$$A_1 = A_3 = -\frac{(B - A) b_s}{2\pi},$$

$$B_1 = -B_3 = \frac{2A b_s}{\pi}$$

$$A_2 = A_4 = -\frac{(B - A)}{2\pi} \frac{G_1(k_2 + 1)}{G_2(k_1 + 1)} b_s,$$

$$B_2 = -B_4 = -\frac{2(1 - A)}{\pi} \frac{G_1(k_2 + 1)}{G_2(k_1 + 1)} b_s \tag{15}$$

Therefore the dislocation distribution functions are completely defined. It is clear from Equation 14 that the array with Burgers vector parallel to the interface is an odd function of y, while the array with Burgers vector perpendicular to the interface is an even function of y. In the above equation, A and B are written in terms of the elastic constants of the two phases; namely, $A = (G_1 - G_2)/(G_1 + G_2 k_1)$ and $B = (G_1 k_2 - G_2 k_1)/(G_1 k_2 + G_2)$. The stress field and the displacement field around the dislocation in the two-phase medium can be obtained by evaluating the Airy stress function in the two media separately. The Airy stress function, $X^{(1)}$ in medium 1 is a result of summing the Airy stress functions of the two arrays in medium 1 over their respective distributions and adding to the Airy stress function of the lattice dislocation. Therefore,

$$X^{(1)} = -\frac{G_1 b_s}{\pi(k_1 + 1)} \left[2y \ln r_1 + \int_{-\infty}^{\infty} (y - y_i) \ln [x^2 + (y - y_i)^2] f_3(y_i)\,dy_i - x \int_{-\infty}^{\infty} \ln [x^2 + (y - y_i)^2] f_1(y_i)\,dy_i \right] \qquad x > 0$$

Evaluation of the integrals provides

$$X^{(1)} = -\frac{G_1 b_s}{\pi(k_1 + 1)} \left[2r_1 \sin\theta_1 \log r_1 - (B + A) r_2 \sin\theta_2 \log r_2 - (B - A) r_2 \theta_2 \cos\theta_2 + 2Ac \left\{ \sin 2\theta_2 - 2c \frac{\sin\theta_2}{r_2} \right\} \right] \qquad x > 0 \tag{16}$$

Similarly the Airy stress function in phase 2 is

$$X^{(2)} = -\frac{G_2 b_s}{\pi(k_2 + 1)} \times \left[\int_{-\infty}^{\infty} (y - y_i) \ln [x^2 + (y - y_i)^2] f_4(y_i)\,dy_i + x \int_{-\infty}^{\infty} \ln [x^2 + (y - y_i)^2] f_2(y_i)\,dy_i \right]$$

$$= -\frac{G_1 b_s}{\pi(k_1 + 1)} [(2 - A - B) r_1 \sin\theta_1 \log r_1 + (B - A) \{ r_1 \theta_1 \cos\theta_1 + 2c\theta_1 \}], \qquad x < 0 \tag{17}$$

where

$$r_1^2 = (x - c)^2 + y^2, \quad r_2^2 = (x + c)^2 + y^2,$$

$$\theta_1 = \tan^{-1}\frac{y}{x-c}$$

and

$$\theta_2 = \tan^{-1}\frac{y}{x+c}$$

Using these Airy stress functions, the stress field and the displacement field around the dislocation in the two phases can be obtained. It is also verified that these results agree with those obtained by the Green's function technique [6] and the image dislocation method [7, 8]. The complete expressions for stresses and displacements are lengthy and therefore will not be included here.

4.2. Edge dislocation with Burgers vector parallel to the interface

The continuity of stresses and displacements across the interface when the edge dislocation with Burgers vector parallel to the interface is considered, as shown in Fig. 5, can be written in terms of the four dislocation distributions. Let $f_1(y)$ and $f_2(y)$ be the dislocation distribution functions representing the surface array whose Burgers vectors, b_{x_i}, are perpendicular to the interface and situated in phases 1 and 2 respectively. Similarly, let $f_3(y)$ and $f_4(y)$ be the dislocation distribution functions representing the surface array whose Burgers vectors, b_{y_i} are parallel to the interface and situated in phases 1 and 2 respectively. Across the interface, the σ_{xy} component due to the surface arrays given by $f_1(y)$ and $f_2(y)$ is zero. Similarly, the σ_{xx} component due to surface arrays $f_3(y)$ and $f_4(y)$ is zero. Therefore, the continuity of the σ_{xx} component can be written in the form,

$$\frac{G_1 b_{x_i}}{\pi(k_1+1)}\int_{-\infty}^{\infty}\frac{f_1(y_1)\,dy_1}{y-y_1} - \frac{G_2 b_{x_i}}{\pi(k_2+1)}\int_{-\infty}^{\infty}\frac{f_2(y_1)\,dy_1}{y-y_1}$$

$$= -\frac{G_1 b_s}{\pi(k_1+1)}\left[\frac{c}{c^2+y^2} - \frac{2c^3}{(c^2+y^2)^2}\right]$$

Inverting the above equation,

$$\frac{G_1 b_{x_i} f_1(y_1)}{(k_1+1)} - \frac{G_2 f_2(y_1) b_{x_i}}{(k_2+1)} = \frac{2G_1 b_s}{\pi(k_1+1)}\frac{c^2 y}{(c^2+y^2)^2} \qquad (18)$$

Similarly, the continuity of the σ_{xy} component can be put into the form,

$$\frac{G_1 b_{y_i}}{\pi(k_1+1)}\int_{-\infty}^{\infty}\frac{f_3(y_1)\,dy_1}{y-y_1} - \frac{G_2 b_{y_i}}{\pi(k_2+1)}\int_{-\infty}^{\infty}\frac{f_4(y_1)\,dy_1}{y-y_1}$$

$$= -\frac{G_1 b_s}{\pi(k_1+1)}\left[\frac{y}{c^2+y^2} - \frac{2c^2 y}{(c^2+y^2)^2}\right]$$

Inverting the above equation

$$\frac{G_1 b_{y_i} f_3(y_1)}{(k_1+1)} - \frac{G_2 b_{y_i} f_4(y_1)}{(k_2+1)} = -\frac{2G_1 b_s}{\pi(k_1+1)}\frac{cy^2}{(c^2+y^2)^2} \qquad (19)$$

The continuity of the U_x component of displacement or the gradient of U_x with y provides

$$b_{x_i} f_1(y_1) + b_{x_i} f_2(y_1) - \frac{(k_1-1)b_{y_i}}{\pi(k_1+1)}\int_{-\infty}^{\infty}\frac{f_3(y_1)\,dy_1}{y-y_1} + \frac{(k_2-1)b_{y_i}}{\pi(k_2+1)}\int_{-\infty}^{\infty}\frac{f_4(y_1)\,dy_1}{y-y_1}$$

$$= \frac{b_s}{\pi}\left[\frac{(k_1-1)}{(k_1+1)}\frac{y}{c^2+y^2} + \frac{4c^2 y}{(k_1+1)(c^2+y^2)^2}\right] \qquad (20)$$

Similarly, continuity of the U_y component of displacement or the gradient of U_y with y provides

$$b_{y_i} f_3(y_1) + b_{y_i} f_4(y_1) + \frac{(k_1-1)b_{x_i}}{\pi(k_1+1)}\int_{-\infty}^{\infty}\frac{f_1(y_1)\,dy_1}{y-y_1} - \frac{(k_2-1)b_{x_i}}{\pi(k_2+1)}\int_{-\infty}^{\infty}\frac{f_2(y_1)\,dy_1}{y-y_1}$$

$$= \frac{b_s}{\pi}\left[\frac{(k_1-1)}{(k_1+1)}\frac{c}{c^2+y^2} + \frac{4cy^2}{(k_1+1)(c^2+y^2)^2}\right] \qquad (21)$$

Equations 18 to 21 can be solved to arrive at the dislocation distributions. The distribution functions can be assumed to be

$$b_{x_i} f_1(y) = A_1\frac{y}{c^2+y^2} + B_1\frac{c^2 y}{(c^2+y^2)^2}$$

$$b_{x_i} f_2(y) = A_2 \frac{y}{c^2 + y^2} + B_2 \frac{c^2 y}{(c^2 + y^2)^2}$$

$$b_{y_i} f_3(y) = A_3 \frac{c}{c^2 + y^2} + B_3 \frac{cy^2}{(c^2 + y^2)^2}$$

$$b_{y_i} f_4(y) = A_4 \frac{c}{c^2 + y^2} + B_4 \frac{cy^2}{(c^2 + y^2)^2} \tag{22}$$

Using Equations 18 to 21 to evaluate the constants provides

$$A_1 = A_3 = -\frac{(B-A)}{2\pi} b_s,$$

$$B_1 = B_3 = -\frac{2A}{\pi} b_s$$

$$A_2 = A_4 = -\frac{(B-A)}{2\pi} \frac{G_1(k_2+1)}{G_2(k_1+1)} b_s,$$

$$B_2 = B_4 = \frac{2(1-A)}{\pi} \frac{G_1(k_2+1)}{G_2(k_1+1)} b_s \tag{23}$$

where the constants A and B are defined as explained earlier. Therefore, the dislocation distributions are completely defined. It is seen from Equations 22 that the distribution functions $f_1(y)$ and $f_2(y)$ are odd functions of y, and hence change their sign along the y axis, while $f_3(y)$ and $f_4(y)$ are even functions of y. The Airy stress functions for the two phases can be written after evaluating the Airy stress functions due to the surface arrays in the two phases. The result for phase 1 is

$$X^{(1)} = \frac{G_1 b_s}{\pi(k_1+1)} \Bigg[2r_1 \cos\theta_1 \log r_1 - (B+A) r_2 \cos\theta_2 \log r_2 + 2Ac \left\{ 2 \log r_2 - \cos 2\theta_2 + 2c \frac{\cos\theta_2}{r_2} \right\} + (B-A) r_2 \theta_2 \sin\theta_2 \Bigg] \tag{24}$$

and for phase 2,

$$X^{(2)} = \frac{G_1 b_s}{\pi(k_1+1)} [(2-A-B) r_1 \cos\theta_1 \log r_1 - 2(B-A) c \log r_1 - (B-A) r_1 \theta_1 \sin\theta_1] \tag{25}$$

As mentioned earlier, the stress field and the disdisplacement field around the dislocation in the two phases can be obtained. Again, the results agree with those obtained by the Green's function technique [6] and the image dislocation method [7, 8]. The complete expressions for stresses and displacement fields are lengthy and therefore will not be included here. When the second phase consists of a vacuum, $G_2 = 0$ and the constants A and B become unity; there will then be only two surface arrays which correspond to those in the semi-infinite medium [10]. When the second phase is rigid, $A = -1/k_1$ and $B = -k_1$. These values can be substituted in the above equations to arrive at the results for the limiting situation. When the two phases possess the same elastic properties, A and B become zero and the above equations for the Airy stress functions become those for the infinite homogeneous medium.

5. Results and discussion

The dislocation distributions and the stress fields obtained earlier indicate that the surface dislocation model can be used to solve the boundary conditions in two-phase media. Here the surface arrays in each medium contribute to the stress field and the displacement field only for the medium in which they are present. It is thus useful to see the effect of these surface arrays on the stress field of the dislocation. Fig. 6 shows the σ_{xz} component of the stress field of a screw dislocation in a two-phase medium where the second phase has a lower shear modulus than phase 1. It is seen that the stress is continuous across the interface. Fig. 7 shows the stress field when the shear modulus of the second phase is larger than that of phase 1. Comparison of these two figures illustrates that the second phase with higher shear modulus increases the stress in the body while the second phase with lower shear modulus decreases the stress in the body. It is seen from Equation 9 that the surface array in phase 1 is of the same sign as that of the lattice dislocation at $(c, 0)$ when $G_2 > G_1$ and it is with opposite sign when $G_2 < G_1$. It becomes obvious from Equations 6 and 7 that the surface array in phase 1 brings an additional term

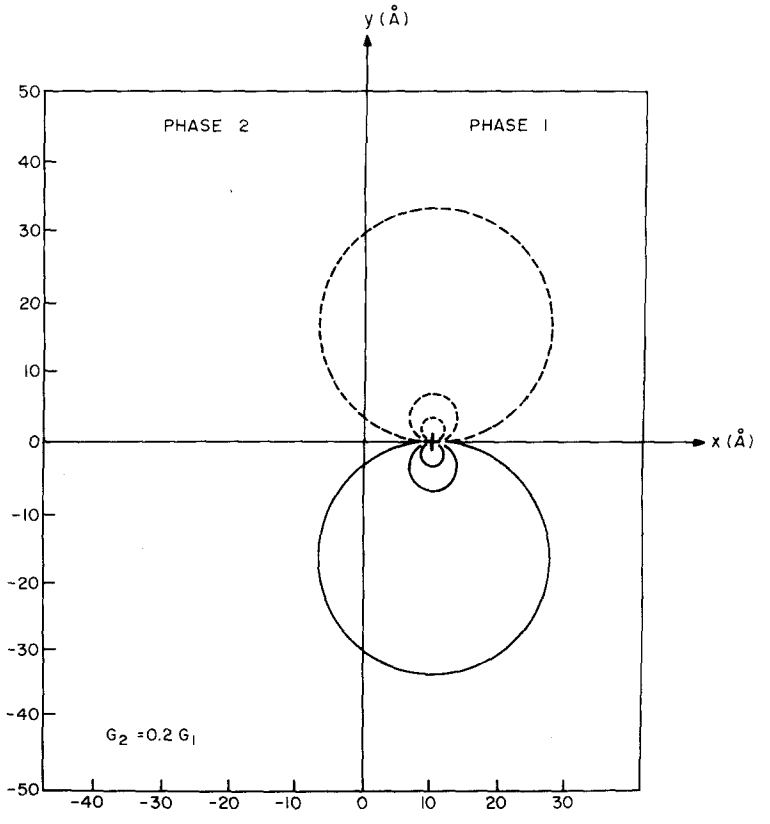

Figure 6 The σ_{xz} component of stress in units of $G_1/2\pi(1-\nu)$ plotted to show the various stress levels of a screw dislocation. The position of the screw dislocation is shown by a plus on the x axis. The dotted lines indicate the negative value of stress and the continuous lines the positive value. A continuous line between a dotted line and a continuous line indicates zero stress level. Starting from the zero stress level, the stress levels correspond to 1×10^{-2}, 5×10^{-2} and 10×10^{-2} on either side for both positive and negative values. Stress contours crossing the interface depart from circularity by amounts too small to be seen.

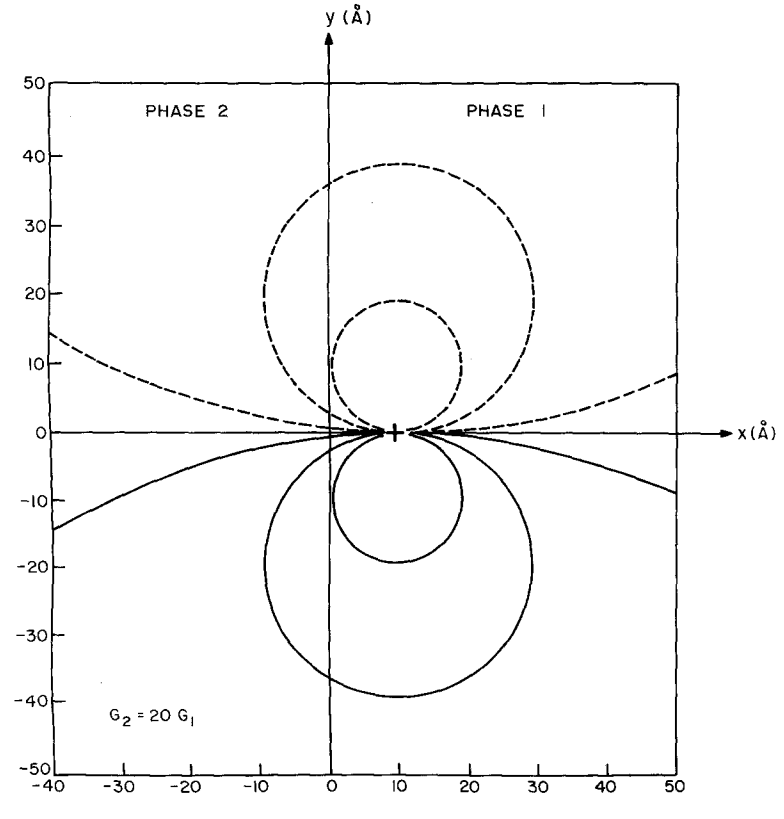

Figure 7 The σ_{xz} component of a screw dislocation with different combinations of shear moduli of the two phases as indicated on the figure. The stress levels are obtained as indicated in Fig. 6. Stress contours crossing the interface depart from circularity by amounts too small to be seen.

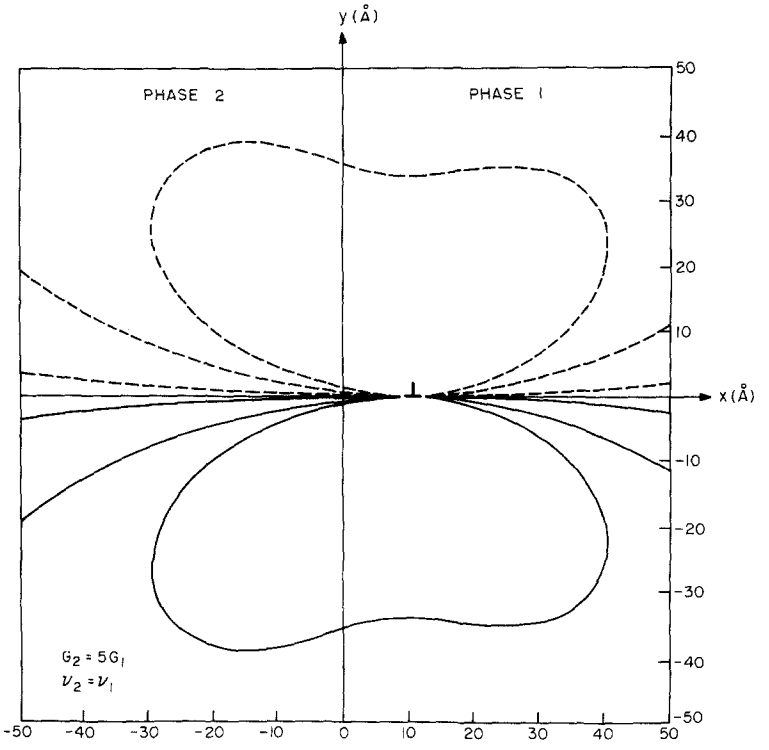

Fig. 8. The Burgers vector of the dislocation is perpendicular to the stress levels of an edge dislocation with Burgers vector perpendicular to the interface. The position of the dislocation is indicated in the figure. The stress levels are obtained as indicated in Fig. 6.

to the stress field of the dislocation in order to match it with that in the second phase. When the second phase is a vacuum, the stress field in the second phase is zero and hence the second term in Equation 6 decreases the stress field of the dislocation at the surface to zero. Therefore, the effect of the surface arrays is to make the stress fields at the internal surfaces equal on both sides, and of a magnitude which decreases with decreasing values of G_2/G_1, down to zero for $G_2/G_1 = 0$. In the image dislocation model, the stress field of the image dislocations serve the purpose of matching the stress components in the two phases.

The stress fields of the edge dislocation with burgers vector perpendicular to the interface and parallel to the interface are more complex due to Poisson's ratio effects which appear in the expressions for the stress and displacement fields. The σ_{xx} component of stress is plotted in Figs. 8, 9 and 10 for three specific situations, namely when $G_2 < G_1$, $G_2 > G_1$ and $G_2 = G_1$ but $\nu_2 < \nu_1$. It is seen from these figures that the stress field becomes symmetric with respect to x but asymmetric with respect to the y axis situated at the centre of the dislocation. When $G_2 > G_1$, the stress fields in medium 2 and medium 1 increase in order to match across the interface. The constants A and B become negative so that in Equations 16 and 17 for the Airy stress functions, the logarithmic terms which are the main contributions to the stress become larger, thus increasing the stress in either phase. When $G_2 < G_1$ and $\nu_2 = \nu_1$ the opposite becomes true. It is seen from Equations 16 and 17 that the asymmetry in the stress field arises due to the stress fields of the surface arrays. When $G_2 = 0$, $A = B = 1$ and X^2 given by Equation 17 becomes zero and the stress vanishes outside the free surface. When $\nu_2 < \nu_1$ but $G_2 = G_1$, $A = 0$ and B is positive so that the logarithmic terms in Equations 16 and 17 become smaller thus decreasing the stress field due to the dislocation in either phase. The surface arrays which are placed in either phase bring the stress fields on the surfaces to the required value. It is important to note that in the formulation of the problem, the distortion in phase 1 is due to the arrays in phase 1 and the lattice dislocation and that in phase 2 is due to the arrays in phase 2. In this respect, the surface arrays are different from the interface dislocations which have distortions in both the phases. The σ_{xy} component of the stress in the two phases is shown in Fig. 11 when $G_2 < G_1$ and $\nu_2 = \nu_1$. It is seen that the stress in the second phase is decreased and therefore the surface array in phase 1 reduces the stress in that phase. When the second phase is a vacuum, the stress in the second phase

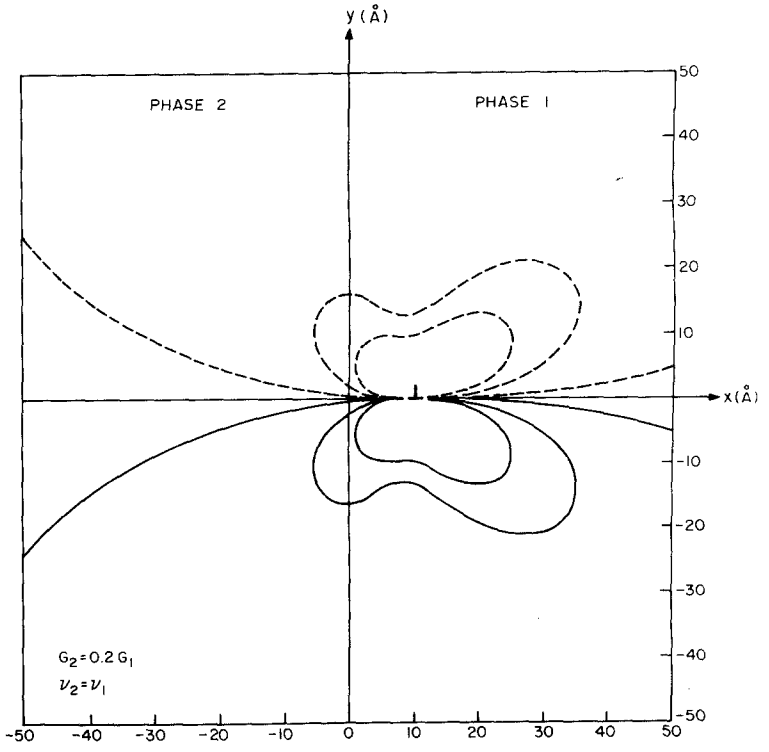

Figure 9 The σ_{xx} component of an edge dislocation in a two-phase medium with different combinations of shear moduli. The stress levels are obtained as indicated in Fig. 8. The Burgers vector of the dislocation is perpendicular to the parallel to the interface.

vanishes completely so that the contours close up on the free surface in phase 1. It has been found that the σ_{xy} component is increased when $G_2 > G_1$ and the same effect of Poisson's ratio is also observed as in the σ_{xx} component. Therefore, these two stress plots are not shown. It should also be noted from Fig. 11 that while the σ_{xy} component is continuous across the interface, the

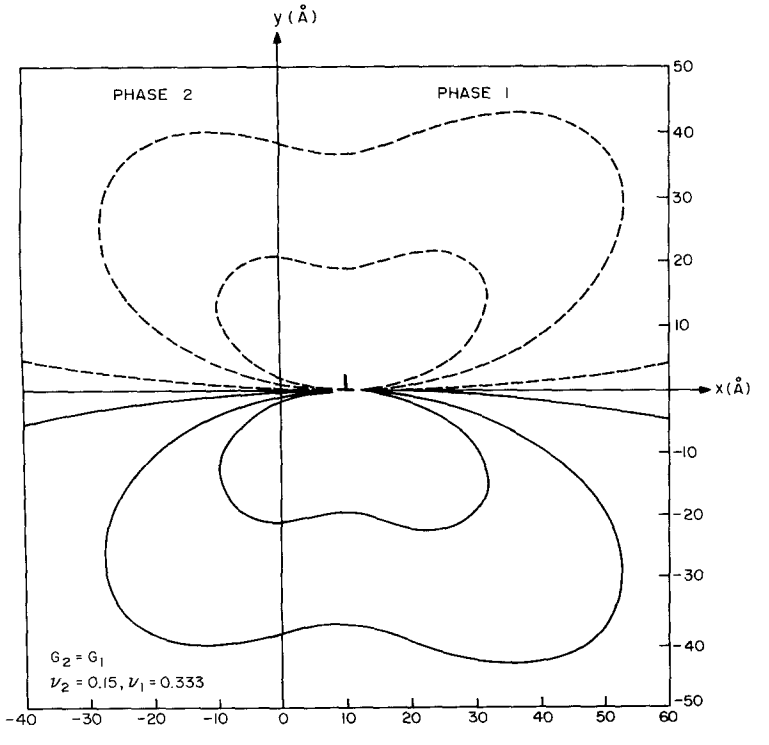

Figure 10 The σ_{xx} component of an edge dislocation in a two-phase medium with different combinations of elastic moduli. The stress levels are obtained as indicated in Fig. 8. The Burgers vector of the dislocation is perpendicular to the interface. The Young's moduli of the two phases are related by $E_2 = 0.863\,E_1$.

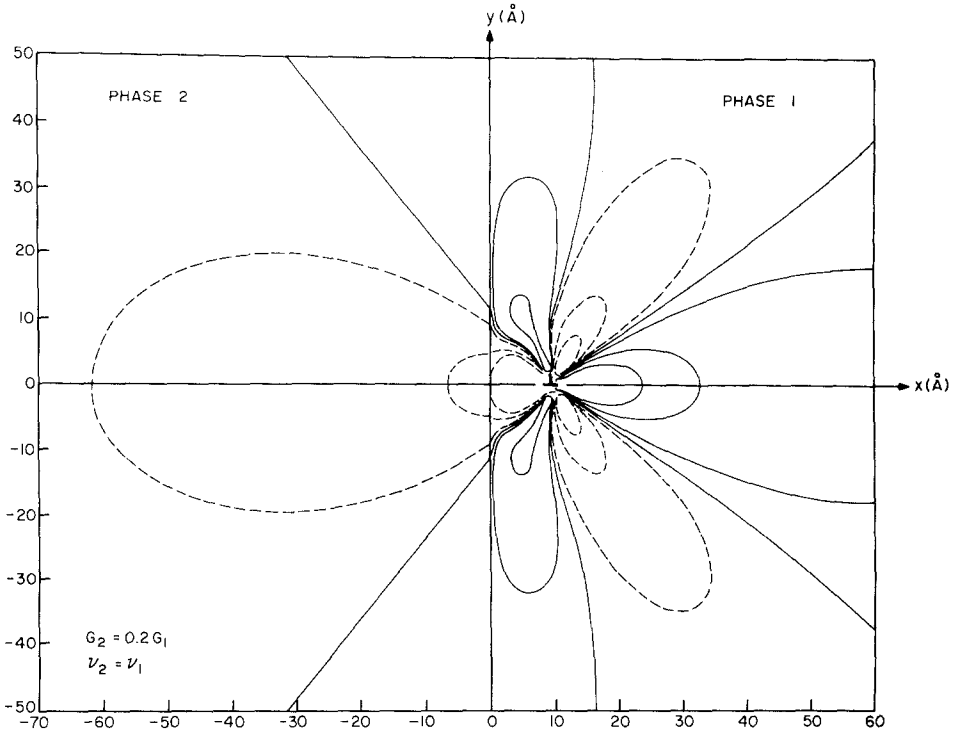

Figure 11 The σ_{xy} component of the stress field of an edge dislocation with Burgers vector perpendicular to the interface. The stress levels are as indicated in Fig. 6. The position of the dislocation is given along the x axis.

slope of the stress contours is different, indicating that the derivative of the stress field need not be continuous.

It is instructive at this point to show in a somewhat more physical way the manner in which the surface dislocation arrays bring about the accommodation of the two-phase interface. In particular, Fig. 12 shows a crystal lattice dislocation situated near the two-phase interface in a finite crystal with Burgers vector normal to the interface, which is

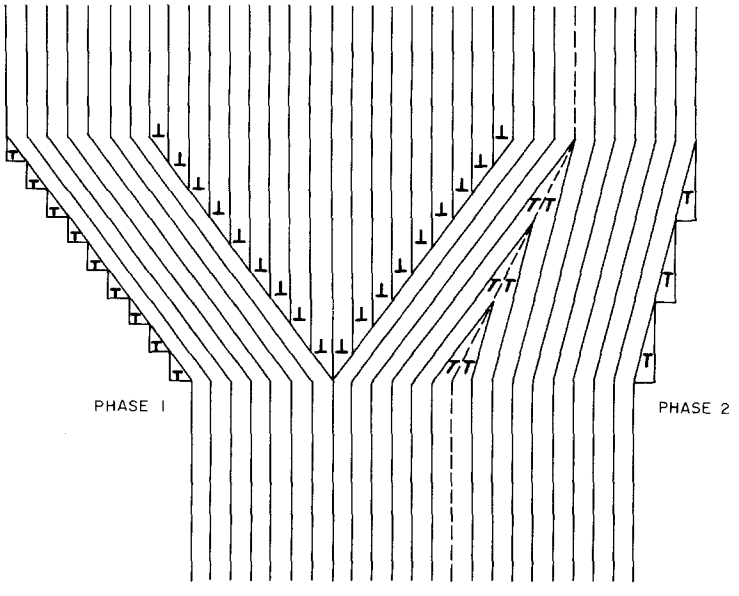

Figure 12 Schematic illustration of an edge dislocation in a finite two-phase medium with Burgers vector perpendicular to the interface. The two phases are depicted in terms of a common lattice where the surface dislocations consist of extra half planes. The lattice dislocation in phase 1 is shown to be spread out and consisting of a large Burgers vector in order to magnify the distortion present in the two phases. The interface is shown dotted and with a large kink, also magnified, to illustrate the distortion. The surface dislocations are in fact located exactly on the interface, although for clarity shown schematically somewhat removed. The surface arrays required to satisfy the free surface boundary conditions are also shown to the far left and right side for each phase. The steps on the free surface indicate the change in the shape of the surface due to relaxation brought about by the surface array.

drawn dotted. For clarity, the Burgers vectors of all dislocations have been normalized to the same value. In particular, the crystal lattice dislocation is seen to be of strength eighteen, i.e. there are eighteen extra half planes associated with this dislocation. It is further assumed that the two phases possess the same lattice parameter. This simplifies the figure in that no additional dislocations need be considered due to a lattice parameter difference. It is seen that the harder second phase toward the right of the interface deforms, i.e. bends less than that of the phase to the left of the interface as indicated by the smaller inclination of the lattice planes. A set of two surface dislocation arrays, i.e. a total of six dislocations, are seen to be required at the interface to provide continuity between the two phases. Two other arrays with Burgers vector parallel to the interface are also required but their contribution is of second order and so as to simplify the figure, they have been omitted. The distortions across the interface have also been magnified in order to show their effects more clearly. Since the two-phase body in Fig. 12 is finite, surface tractions exist in both the right- and left-most vertical faces. These surface tractions can be removed by the addition of a set of surface dislocations in much the same way as they served to satisfy the boundary conditions at the two-phase interface. Again for simplicity, a second set of surface dislocations with Burgers vector parallel to the free surface have been omitted since they are of secondary importance. A detailed discussion of the nature of these surface arrays and their effect on the shape of the surface has been given elsewhere [10]. They, in fact, represent a special case of the present problem in which one of the phases consists of a vacuum. It will be noted that the right-hand face contains three surface dislocations whereas the left-hand face is comprised of nine such dislocations. It is also to be observed that a powerful conservation law is to be followed here, namely that the sum of the Burgers vectors of the surface and crystal dislocations should add up to zero. This is clearly seen in Fig. 12 where the crystal lattice dislocations of strength eighteen is just balanced by the eighteen surface dislocations which have Burgers vectors of opposite sign. In terms of elastic properties, the second phase towards the right of the dotted line in Fig. 12 is harder than phase 1 and assuming $\nu_2 = \nu_1$, B and A in Equation 15 become negative with $B > A$, which accounts for the fact that the Burgers vectors of the surface arrays are of opposite sign to that of the lattice dislocation. It follows that in the present analysis, since the two half spaces associated with the two phases are semi-infinite, the free surface dislocation arrays need not be considered. The above physical interpretation of the surface dislocation model for a dislocation near a two-phase interface is useful in employing numerical techniques where the surface arrays are assumed to be discrete dislocations. Such discrete dislocation analysis, although not performed here for the finite two-phases system, gave results which are close to those obtained by the continuous distribution method in the case of a semi-infinite solid containing a dislocation [10].

It is interesting to observe the shape of the interface when the dislocation comes closer to the interface. This is obtained by plotting the U_x component of displacement, as shown in Figs. 13a and b for two values of the shear modulus of the second phase. When $G_2 < G_1$, the shape of the surface is similar to that of a ledge formed on the free surface of a body when the dislocation comes close to the surface. Fig. 13a shows the shape of the interface when the dislocation approaches the interface. The shape of the interface shown in Fig. 13b when $G_2 > G_1$ is different in that the interface changes the sign of its curvature as one moves away from the dislocation in the y direction. The difference in the variation of U_x for the two situations illustrated in Figs. 13a and b is difficult to explain physically. The displacement component is obtained from the two dislocation distributions in each phase with an additional contribution to the displacement in phase 1 from the lattice dislocation in phase 1. It has been found that the distribution function representing the surface dislocations with Burgers vector parallel to the interface in phase 1 changes sign once along one half of the y axis. It is also noted that this distribution is an odd function of y. Thus, the distribution changes sign three times along the y axis. This variation of the distribution function with proper combination of the shear moduli $G_2 > G_1$ is expected to give the U_x component of displacement shown in Fig. 13b.

The σ_{xx} and σ_{xy} components of the stress field of a dislocation with Burgers vector parallel to the interface are plotted in Figs. 14 and 15 respectively when the second phase has a lower shear modulus than that of the phase 1. It is seen from these figures that the stress field is reduced by the

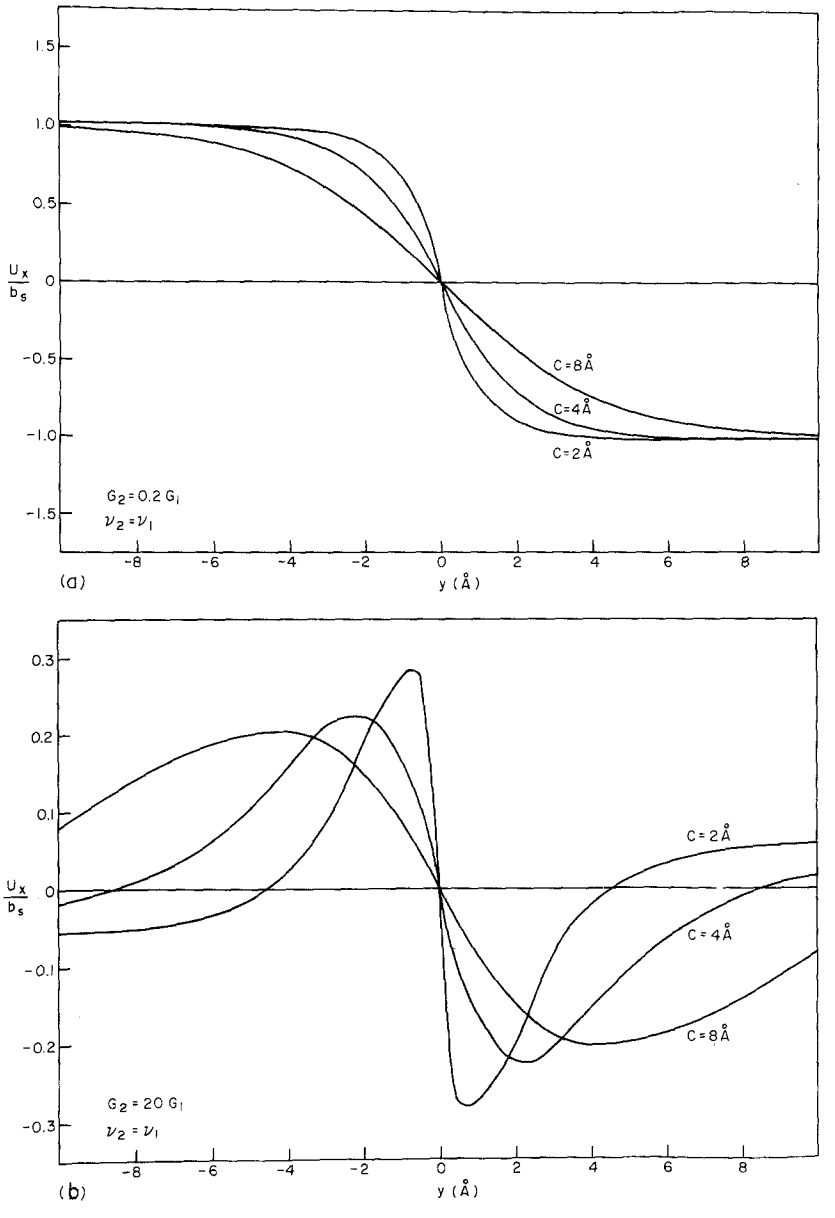

Figure 13 (a) The U_x component of displacement along the interface shown to indicate the shape of the interface when $G_2 < G_1$ and $\nu_2 = \nu_1$. The displacement is given in units of half the Burgers vector of the dislocation. The Burger's vector is normal to the interface. (b) The U_x component along the interface shown to indicate the shape of the interface when $G_2 > G_1$ and $\nu_2 = \nu_1$. The displacement is given in units of half the Burgers vector of the dislocation. The Burgers vector is normal to the interface.

second phase. In the limiting situation when the second phase is a vacuum, the stress contours close up along the free surface. The stress field is continuous but the derivative of the stress is not continuous, as indicated by the change of slope of the curves. The general conclusions regarding the effect of the elastic properties of the second phase on the stress plots remains the same as those observed for a dislocation with Burgers vector perpendicular to the interface. Therefore, the stress plots for situations when $G_2 > G_1$ and $G_2 = G_1$ and $\nu_2 < \nu_1$ are not shown separately. When the second phase is rigid compared to the matrix, the stress levels approach a limiting value indicating that it is the highest value possible everywhere for the combination of the two phases.

The distortion across the interface due to a dislocation with Burgers vector parallel to the interface is shown in Fig. 16 indicating the surface dislocation arrays in the two phases. The crystal lattice dislocation is situated in the lower half space where the interface is shown by a dotted line. Similar to the case of Fig. 12, only the primary array of dislocations in the surface arrays are shown everywhere. It is seen from Fig. 16 that the harder phase which is below the dotted line bends less than that of the second phase above the interface as indicated by the smaller inclination of the

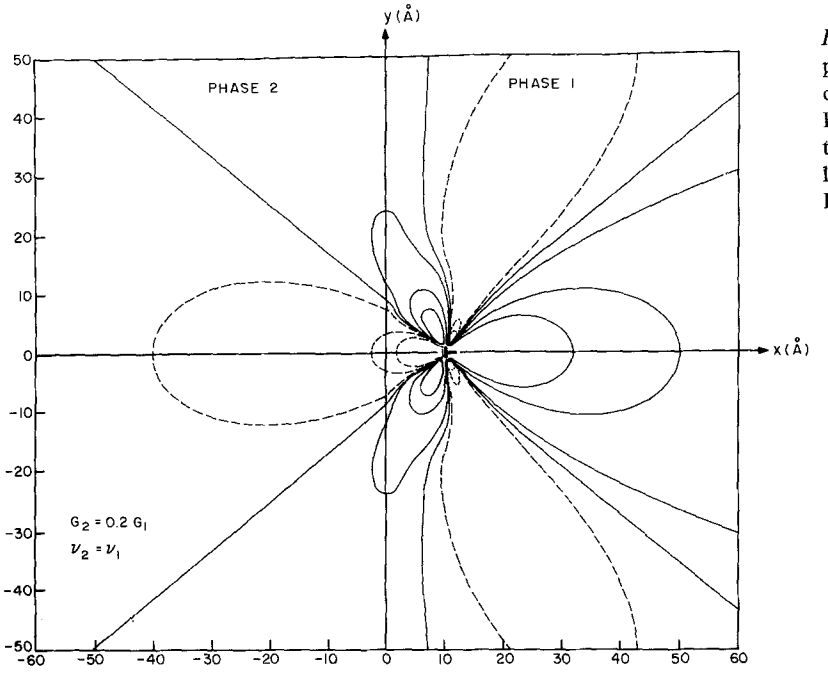

Figure 14 The σ_{xx} component of the stress field of an edge dislocation with Burgers vector parallel to the interface. The stress levels are as indicated in Fig. 6.

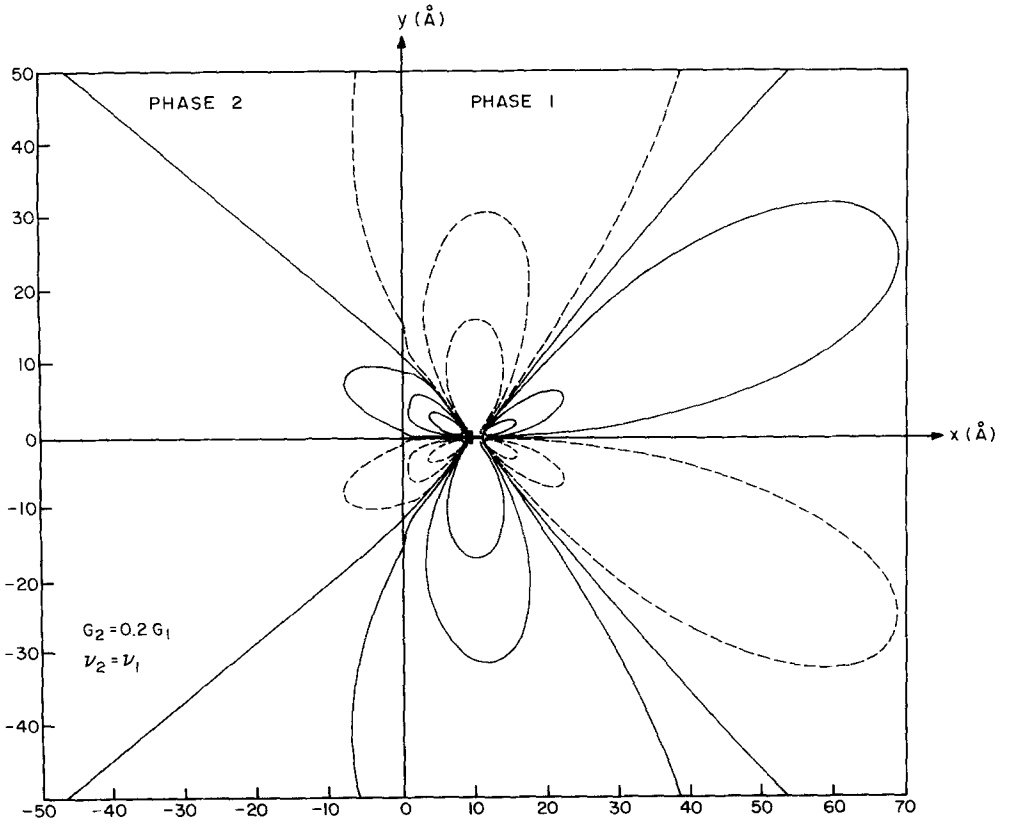

Figure 15 The σ_{xy} component of the stress field fof an edge dislocation with Burgers vector parallel to the interface. The stress levels are as indicated in Fig. 6. The position of the dislocation is shown along the positive x axis.

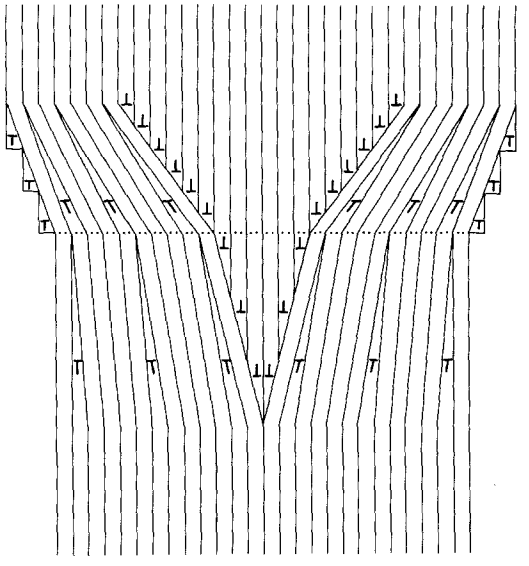

Figure 16 Schematic illustration of an edge dislocation in a finite two-phase medium with Burgers vector parallel to the interface. The two phases are shown in terms of a common lattice where the surface dislocations consist of extra half planes. The lattice dislocation in phase 1 is shown to be spread out and consisting of a large Burgers vector in order to magnify the distortion present in the two phases. The severe distortion due to the dislocation enters phase 2. The interface is shown dotted without a kink or bend in order to avoid the presence of other dislocations and thus avoid confusion. The surface dislocations are present exactly at the interface, although for clarity they are shown somewhat removed. The surface arrays required to satisfy the free surface boundary conditions are also shown on far left and right sides for each phase. The steps on the free surface indicate the change in the shape of the surface due to relaxation brought about by the surface array.

lattice planes. A detailed discussion of Fig. 16 follows the same reasoning as that for Fig. 12 and hence it is not included here. Fig. 16 forms the basis for the discrete dislocation model of a dislocation with Burgers vector parallel to the interface which can be analysed numerically.

The surface dislocation model of interface boundary conditions shows that this method can be applied to the two-phase systems without having to solve the basic elasticity equations needed to satisfy the continuity conditions. Thus, the method is relatively simple and involves no mathematical complexity. The surface arrays also indicate as shown in Figs. 12 and 16, the distortion across the interface in both the phases. Since, each array in the interface belongs to only one medium in which it is present, the two phases can be separated and the distortion is completely accounted for by the arrays. The other two methods, hitherto used in the literature to satisfy the interface boundary conditions, namely the Green's function method and the image dislocation model, do not have the above-mentioned advantage. Also, when the two-phase medium is finite in size, the free surface boundary conditions should also be satisfied in addition to the internal surface boundary conditions. While the surface dislocation model may be employed using the discrete dislocation approach [10], the other two methods cannot be used as effectively as the present model to deal with the additional boundary conditions.

6. Discrete dislocation method

The surface dislocation model is employed to solve the continuity conditions across the interface using the continuous dislocation distribution method. The dislocation distribution is further used to arrive at the Airy stress functions in the two media. When the interface possesses a complex geometry and the two-phase medium is finite, the method of continuous distribution of dislocations may also be cumbersome due to complex integral equations which should be inverted to obtain the distribution functions. In those cases where the analysis becomes difficult, it has been shown that the discrete dislocation method can be used very efficiently [10]. In this method of analysis, the continuous distribution is replaced by discrete dislocations and instead of using the stress fields and the displacement fields, the total energy of the configuration is minimized with respect to the positions of the discrete dislocations. It has been shown that the discrete dislocation method can be used to satisfy the boundary conditions to any accuracy required by choosing the required number of dislocations. However, this method can be applied only to those situations where the energy of the configuration is not infinite, i.e., it can only be applied where the stress field of the configuration is short range*. In the present analysis where the stress field of the dislocation in the two-phase medium composed of two semi-infinite half spaces is long range, this method cannot be applied since the energy of the configuration is also infinite. But the method

* The authors have subsequently applied the discrete dislocation method to two-phase systems [14].

becomes useful when the two-phase medium is finite in dimensions [14].

7. Summary and conclusions

The surface dislocation model has been utilized to satisify the continuity conditions across the planar interface of a two-phase medium composed of two semi-infinite half spaces containing a dislocation in one of the phases. The three fundamental orientations of the Burgers vectors of the dislocations are considered and analysed completely to obtain the stress field and the displacement field in the two media. The stress fields are plotted for the three orientations to show the effect of the shear modulus of the second phase on the variation of the stress in the two-phase region. It is shown that a second phase with lower shear modulus reduces the stress field, while the opposite is true when the second phase has higher shear modulus. In the extreme situation when the second phase is a vacuum, the stress levels close along the free surface. Also, the stress reaches a maximum level everywhere when the second phase is very rigid. The effect of decreasing Poisson's ratio is the same as decreasing the shear modulus, although the two have different magnitude effects on the stress field. The distortion across the interface that arises due to the dislocation is shown in the two specific situations where the Burgers vector is either perpendicular to the interface or parallel to it. The advantages of the surface dislocation model over the other two methods, namely, its simplicity of analysis and its ability to solve complex problems with relative ease, are discussed. The surface arrays across the interface are shown to indicate the distortion across the interface of the two phases. The surface arrays are different from the interface array since the distortion due to the surface dislocations exists only in the medium in which they are present while the distortion due to the interface array is present in both phases. The advantages of the surface dislocation model in applying the discrete dislocation method to the finite two-phase medium with curved interfaces is mentioned and its limitations for the long range stress problems are also indicated.

Acknowledgements

The computer time for this project was supported in full through the facilities of the Computer Science Center of the University of Maryland. Financial support for the present study was provided by the U.S. Department of Energy under Contract No. AT-(40-1)-3935.

References

1. J. H. MICHELL, *Proc. Lond. Math. Soc.* **31** (1899) 100.
2. R. DeWIT, *Solid State Phys.* **10** (1960) 249.
3. J. M. BURGERS, *Proc. Kon. Ned. Akad. Wetenschap.* **42** (1939) 293.
4. J. DUNDURS and M. HETENYI, *J. Appl. Mech.* 28 (1961) 103.
5. *Idem ibid.* **29** (1962) 362.
6. T. MURA, "Advances in Materials Research", edited by H. Herman (Interscience, New York, 1968).
7. A. K. HEAD, *Phil. Mag.* **49** (1953a) 92.
8. *Idem, Proc. Phys. Soc. (Lond)* **B66** (1953b) 793.
9. J. WEERTMAN, "Elementary Dislocation Theory", edited by M. E. Fine (MacMillan, New York, 1964).
10. K. JAGANNADHAM and M. J. MARCINKOWSKI, *Phys. Stat. Sol.* **50A** (1978) 293.
11. *Idem, J. Appl. Phys.* **48** (1977) 3788.
12. *Idem, Mater. Sci. Eng.* **38** (1979) 259.
13. J. P. HIRTH and J. LOTHE, "Theory of Dislocations" (McGraw Hill Co., New York, 1968).
14. K. JAGANNADHAM and M. J. MARCINKOWSKI, *Mater. Sci. Eng.* (to be published).

Received 28 March and accepted 11 May 1979.